Cyclin E Overexpression Obstructs Infiltrative Behavior in Breast Cancer: A Novel Role Reflected in the Growth Pattern of Medullary Breast Cancers

Pontus Berglund,[1] Maria Stighall,[1] Karin Jirström,[1] Signe Borgquist,[1] Anita Sjölander,[2] Ingrid Hedenfalk,[1] and Göran Landberg[1]

Divisions of [1]Pathology and [2]Experimental Pathology, Department of Laboratory Medicine, Lund University, Malmö University Hospital, Malmö, Sweden

Abstract

Cell cycle deregulation is a prerequisite in tumor development and overexpression of cyclin E, a major G_1-S regulator, is often observed in breast cancer and is further linked to poor prognosis. By overexpressing cyclin E in a retinoblastoma-inactivated breast cancer cell line, we induced significant alterations in the expression of genes associated with proliferation and cell adhesion. Rearrangements of the actin cytoskeleton in addition to increased adhesive properties, decreased motility, and invasive potential in functional assays, indicated an overall abrogated mobility. Consistent *in vivo* findings were obtained upon investigation of 985 primary breast cancers, where cyclin E–high tumors predominantly (67%) displayed a low infiltrative, pushing growth pattern. Furthermore, medullary breast cancers, a subtype defined by its pushing, delimited growth, exhibited a remarkable frequency of cyclin E deregulation (87%) compared with other histologic subtypes (5-20%). Taken together, our results suggest the novel role of cyclin E in modeling infiltrative behavior. The consequences of cyclin E overexpression in breast cancer seems to be multiple, including effects on proliferation as well as growth patterns, a scenario that is indeed observed in the archetype of cyclin E–overexpressing medullary breast cancers. (Cancer Res 2005; 65(21): 9727-34)

Introduction

Breast cancer is one of the leading causes of cancer death among women in the Western world. Many different forms of breast cancer exist, with a multitude of clinical appearances ranging from a rather indolent disease without metastases to rapidly progressing and highly proliferative tumors with extremely aggressive behavior. The growth pattern of breast tumors is one characteristic that varies, where some tumors display a clear infiltrative growth pattern with sieving tumor cells at the edges, whereas others have a more solid growth pattern with large pushing tumor fronts. The presence of a pushing margin is a common morphologic feature of estrogen receptor–negative tumors and has been associated with negative lymph node status (1). Invasive breast tumors are classified into several histologic types, where ductal carcinomas make up the majority and lobular and medullary breast carcinomas are two noteworthy but less frequent types. The different histologic types of breast cancer have specific morphologic characteristics and differ to some extent regarding prognosis (2). Tumor type and in particular differentiation grade, therefore influence clinical treatment decisions, whereas expression of hormone receptors (estrogen receptor and progesterone receptor) as well as the C-erbB2 are important predictive markers for endocrine and trastuzumab treatment responses, respectively.

High protein levels of cyclin E, an activating subunit of cyclin-dependent kinase 2 (CDK2), is often observed in breast cancer and is strongly linked to poor prognosis (3). Deregulation of cell cycle control is thought to be a prerequisite in tumor development and several studies have shown an accelerated S phase entry due to constitutive expression of cyclin E (4, 5). Furthermore, cyclin E is able to induce chromosome instability by inappropriate initiation of DNA replication and centrosome duplication (6, 7). Transgenic mice expressing elevated levels of cyclin E in the mammary epithelium during pregnancy and lactation suffer from a higher incidence of mammary adenocarcinoma (8), suggesting that cyclin E might act as an oncogene in this tissue (9). Collectively, several lines of evidence indicate that deregulated expression of cyclin E affects important properties in tumor development.

A general concept emerging from the different fields of cancer research is the existence of cross-talk between various signaling pathways, indicating links between cellular activities. Thus, many tumor-related properties might be interconnected and either enforce or counteract each other. In this study, we therefore wanted to delineate the downstream effects of overexpressed cyclin E, aiming at investigating whether cyclin E expression has an effect on other cellular functions besides proliferation, relevant to tumor development and behavior such as apoptosis, invasion, or angiogenesis. In summary, we observed that cyclin E overexpression induced differences in gene expression patterns associated with cell adhesion as well as increased adhesive capacity and reduced ability to migrate and invade in functional assays. The results were further validated in a large sample of primary breast cancers, where infiltrative tumor growth was inversely associated with cyclin E protein levels. Our results imply a novel role for cyclin E in affecting tumor growth patterns, in addition to its well-established function in controlling cell proliferation.

Materials and Methods

Cell culture. All experiments were carried out using the breast cancer cell line MDA-MB-468 (ATCC, Int., Manassa, VA). The cells were cultured in RPMI 1640 supplemented with 10% FCS, sodium pyruvate (1 mmol/L), streptomycin (18 μg/mL), and penicillin (18 IU/mL).

Requests for reprints: Göran Landberg, Division of Pathology, Department of Laboratory Medicine, Lund University, Malmö University Hospital, 20502 Malmö, Sweden. Phone: 46-4033-1953; Fax: 46-4033-7063; E-mail: goran.landberg@med.lu.se.

doi:10.1158/0008-5472.CAN-04-3984

Vectors. The wild-type cyclin E vector construct used was a kind gift from Dr. Geisen at The Burnham Institute, La Jolla, CA. cDNA for cyclin E (human origin) was PCR-amplified from pBluescript constructs with primers generating 3′-ends without stop codons. The modified cyclin E cDNA (1-395 amino acids) was subsequently cloned into a pEGFP-N3 plasmid (Clontech, Mountain View, CA), creating a COOH-terminal fusion gene with enhanced green fluorescent protein (EGFP). A pEGFP-C2 plasmid (Clontech) was used as a control vector, expressing only EGFP. The expression of the fusion gene and the EGFP gene from the respective vectors was under the control of the cytomegalovirus promoter.

Transfections. Transfectants were obtained by electroporation using protocol and equipment from Amaxa Biosystem (Cologne, Germany). The cells were propagated to ~80% confluency with a medium change 1 day before transfection. For every transfection, 1×10^6 cells were trypsinized and centrifuged and subsequently dissolved in 100 μL Nucleofector Solution (Kit V). Vector DNA (5 μg) was added and the cells were electroporated immediately using transfection program Q-28. The transiently transfected cells were harvested and analyzed 24 hours after transfection. To obtain stable clones, the transfected cells were cultured in normal medium for 48 hours and thereafter in selective medium containing G418 (500 μg/mL). Collections of stable transfectants were guided by EGFP fluorescence and protein expression was confirmed by Western blotting. The selected clones were subsequently propagated in medium supplemented with G418 (100 μg/mL).

Flow cytometry. The cells were trypsinized and fixed with 70% ethanol for 20 minutes at −20°C. After fixation, the cells were washed with PBS and centrifuged. The pellets were subsequently dissolved in Vindelöv solution [3.5 μmol/L Tris-HCl (pH 7.6), 10 mmol/L NaCl, 50 μg/mL propidium iodide, 20 μg/mL RNase, 0.1% v/v NP40] and incubated in the dark for 20 minutes on ice, in order to stain the DNA. The analysis was carried out with FACScalibur and Cellquest software (BD Biosciences Immunocytometry Systems, San Jose, CA), counting in total 1×10^4 cells. Gating of G_0-G_1-, S- and G_2-M-populations was done manually using WinList software (Verity Software House, Inc., Topsham, ME). When analyzing the transiently transfected population, a gate was used discriminating the transfected EGFP-positive cells from the untransfected cells.

Western blotting and immunoprecipitation. Transfected cells were washed and scraped off in fresh PBS. After centrifugation, the pellets were dissolved and vortexed in lysis buffer [0.5% NP40, 0.5% NaDOC, 0.1% SDS, 50 mmol/L Tris (pH 7), 150 mmol/L NaCl, 1 mmol/L EDTA (pH 8), 1 mmol/L NaF, 0.1 mg/mL phenylmethylsulfonyl fluoride, protease inhibitor cocktail tablet from Roche (Indianapolis, IN)]. Lysates used in the immunoprecipitation were extracted with radioimmunoprecipitation assay buffer [0.5% NaDOC, 0.5% Triton X-100, 50 mmol/L Tris-HCl (pH 7), 150 mmol/L NaCl, 25 mmol/L NaF, 1 mmol/L $Na_4P_2O_7$, 0.1 mg/mL phenylmethylsulfonyl fluoride, protease inhibitor cocktail tablet from Roche]. The cell extracts were incubated on ice for 30 minutes, centrifuged at 14,000 rpm for 30 minutes, and the supernatants were collected. Protein concentrations were measured by use of the Bicinchoninic Acid Protein Assay (Pierce, Rockford, IL). For Western analysis, 20 μg of protein were loaded and separated on 12% SDS-PAGE gels, and transferred onto cellulose membranes (Hybond ECL, Amersham Pharmacia Biotech, United Kingdom). The membranes were blocked with PBS containing 5% dried milk and 0.05% Tween 20, and then probed with antibodies against cyclin E (1:500 HE12, Santa Cruz Biotechnology, Santa Cruz, CA), E-cadherin (1:500 33-4,000, Zymed, South San Francisco, CA), β-catenin (1:1,000 C2206, Sigma-Aldrich, St. Louis, MO), and actin (1:500 I-19, Santa Cruz), and subsequently visualized using the enhanced chemiluminescence system (Amersham). In the immunoprecipitation assay, 600 μg protein was incubated for 2 hours with 2 μg E-cadherin antibody and 40 μL protein G sepharose beads (Amersham). Fetal bovine serum was used as a negative control in the immunoprecipitation of E-cadherin. The precipitated proteins were subsequently separated from the sepharose beads, run on a 12% SDS-PAGE gel, transferred and probed against E-cadherin, β-catenin, and actin.

Oligonucleotide microarray analysis. RNA from the cyclin E clone pair (A10 and B6) and the control clone pair (B12 and G10) was extracted using TRIzol (Life Technologies Inc., Rockville, MD) and the RNeasy Midi Kit (Qiagen, Valencia, CA). The clone pair RNAs were subsequently pooled, reverse-transcribed, and labeled using the Pronto! Plus Direct Labelling v1.2 system (Corning Inc., Corning, NY). The hybridization was carried out twice and control clone cDNA was used as reference in the analysis. The output intensity raw data was uploaded to the BioArray Software Environment (10) and quality-filtered by excluding spots with a signal-to-noise ratio <2. Out of 55.488 spots available on the slides, 25.977 and 23.183 spots (representing 13.869 and 12.581 reporters) passed the filtering criteria in hybridization 1 and 2, respectively. The filtered data was subsequently normalized using the PIN-based locally weighted scatterplot smoothing algorithm. The final set of 434 genes that were assigned as differentially expressed in the cyclin E–overexpressing clones and further used in the GoMiner analysis, were obtained by including genes (*a*) whose fold induction or repression was greater than or equal to two (in total 2.547 reporters of 14.851 represented), (*b*) with signal present from both hybridizations represented at least by one spot per slide (962 reporters of 2.547), and (*c*) with ascribed gene symbols (434 reporters of 962). The cutoff level was based on self-self hybridizations using cDNA obtained from untransfected MDA-MB-468 cells. The fold changes presented for thrombospondin 1 (*THBS1*), paxillin (*PXN*), and matrix metalloproteinase 7 (*MMP7*) are mean values of the ratios from the respective signal-generating spots. Custom-made oligonucleotide microarray slides containing 55,488 spots representing ~17,500 unique genes in addition to expressed sequence tags, in duplicate, were obtained from the SWEGENE DNA Microarray Resource Center at the BioMedical Center B10 in Lund, supported by the Knut and Alice Wallenberg foundation through the SWEGENE Consortium. The microarray procedure and image analysis were carried out as described in the MIAME Checklist (Supplemental procedure), and the microarray raw data are available from ArrayExpress database (http://www.ebi.ac.uk/arrayexpress/) with accession number E-MEXP-339.

Attachment, motility, and invasion assays. Attachment assays were done by seeding 1×10^5 cells/well, five wells/clone [cyclin E (cyE)-A10, cyE-B6, EGFP-B12, EGFP-G10], in 96-well culture plates. The cells were then allowed to adhere to the surface for 1 hour. Nonadherent cells were removed by rinsing with PBS and the remaining adherent cells were incubated with MTS-solution (CellTiter 96 AQ_{ueous} One Solution cell proliferation assay, Promega, Madison, WI; diluted 1:5 with serum-free RPMI medium) for 1.5 hours. The metabolically active cells reduced the dye to formazan, and absorbance was measured using a Fluostar microplate reader (544 nm excitation filter; BMG Lab Technologies, Offenberg, Germany), quantifying the amount of attached cells. The adhesion experiment was repeated five times. Scratch assays were conducted in triplicate by plating cells in slide chambers, and allowing them to reach confluency. Scratches were made using a sterile pipette tip and photographs were taken after 48 hours with ×10 magnification. Invasion assays were done with BD Biocoat Matrigel Invasion chambers (24-well format). The two clones of cyclin E (A10 and B6) and control transfectants (B12 and G10) were pooled, respectively, and 500 μL serum-free medium containing 8×10^4 cells of each pool were added to the Boyden chambers and allowed to invade for 20 hours at 37°C. Medium (750 μL) supplemented with 10% fetal bovine serum were placed in the wells beneath the chambers to act as a chemoattractant. Invading cells were subsequently fixed in 4% paraformaldehyde for 10 minutes, stained with 1% toluidine blue for 2 minutes, and manually counted. The invasion assay was done twice, plating cells in triplicate, and averages of total number of invading cells/chamber were calculated. To estimate the invasive potential of the transiently transfected cells, $\sim 8 \times 10^4$ cells were immediately transferred from the electroporation cuvette onto the Boyden chambers. The remaining transfected cells were seeded on glass slides. The invading cells and the cells grown on glass slides were stained after 24 hours with 4′,6-diamidino-2-phenylindole. The transfected, EGFP-positive, cells were counted using a fluorescence microscope and the percentage of transfected cells were calculated. Dividing the percentage of transfected cells among the invading cells with the percentage of transfected cells among the glass-grown cells resulted in a ratio used as a measure of the relative invasiveness of the cyclin E- and control-transfected cells. This experiment was repeated seven times, generating mean values of the proportion of transfected cells that did invade. Student's *t* test was used to calculate *P* values.

Tissue microarray and immunohistochemistry. The tissue microarrays were constructed using one tumor sample consisting of 500 tumors from premenopausal women and two samples of mixed pre- and postmenopausal tumors (n = 450 and n = 540). Relevant core sections from ~66% of all cases were obtained, enabling analysis of 985 tumors. All tumor samples were formalin-fixed, paraffin-embedded surgical breast tumor specimens archived at the Department of Pathology, Malmö University Hospital, Sweden. The study was approved by the ethics committee at Lund University, Sweden. In brief, two 0.6-mm cores were taken from selected areas in each donor block and mounted in a recipient block containing between 200 and 300 biopsies. For immunohistochemistry, 6 μm sections of the paraffin-embedded tissue arrays were dried, deparaffinized, rehydrated, and microwave-treated for 10 minutes in an EDTA buffer (pH 8.0). The array sections were subsequently processed in an automatic immunohistochemistry staining machine (Techmate 500, DAKO, Copenhagen, Denmark) for cyclin E (1:100 HE12; Santa Cruz). The premenopausal samples were further stained for Ki67 (1:200, M7240, DAKO; Techmate 500, DAKO), estrogen and progesterone receptor, and HER2. The latter three proteins were analyzed using the Ventana Benchmark system (Ventana Medical Systems Inc., Tuczon, AZ), with prediluted antibodies (anti-estrogen receptor clone 6F11, anti-PgR clone 16, and pathway CB-11 760-2694, respectively). *HER2* gene amplification was determined by fluorescence *in situ* hybridization using an automated staining procedure according to the manufacturer's recommendations (Ventana Medical Systems). Pretreated and denatured tumor sections were incubated overnight with the hybridization probe and subsequently counterstained and evaluated for *HER2* gene copy number using a fluorescence microscope at a magnification of ×40. The stable clones were harvested, formalin-fixed, and paraffin-embedded and organized in a cell microarray. The array was processed (Techmate 500, DAKO) and stained against p27 (1:200, DAKO) and *THBS1* (1:250 N-20, Santa Cruz).

Tumor growth pattern assessment. By studying whole H&E-stained sections, two independent investigators (P. Berglund and K. Jirström) assessed the overall growth characteristics of each tumor. The growth patterns were divided into four groups defined by the mode of infiltration, from a "sieving" and diffuse infiltration to a clearly pushing growth pattern with well-defined margins. In addition to the extreme groups exhibiting an exclusive infiltrative or pushing pattern, two intermediary groups were used to account for the tumors with predominantly infiltrative or predominantly pushing growth. In total, 221 tumors were analyzed and assigned to one of the four groups.

Phalloidin staining. Cells were fixed with 4% paraformaldehyde in PBS for 4 minutes, permeabilized, and blocked with 5% normal goat serum and 0.3% Triton X-100 in TBS for 30 minutes. Filamentous actin (F-actin) was stained for 20 minutes with Alexa Fluor 546-conjugated phalloidin (Molecular Probes, Eugene, OR) diluted 1:100 in TBS.

Cell fractionation and assessment of membrane-bound RhoA, Rac1, and Cdc42. Stable clones were rinsed with PBS and covered with buffer A [20 mmol/L Na-Hepes (pH 8.0), 2 mmol/L $MgCl_2$, 1 mmol/L EDTA, 5 mmol/L orthovanadate, 60 μg/mL phenylmethylsulfonyl fluoride, and 4 μg/mL leupeptin] and placed on ice, scraped off and subsequently homogenized with a Dounce homogenizer. Cell suspensions were centrifuged at 200 × g to remove intact nuclei. The supernatant was centrifuged at 10,000 × g for 10 minutes and the resulting supernatant was separated into cytosol and plasma membrane fractions by centrifugation at 200,000 × g for 1 hour. The resulting membrane pellet was suspended in buffer A. The levels of membrane-associated RhoA, Rac1, and Cdc42 were assessed by Western analysis of the plasma membrane fractions, 20 μg protein/clone, using the following antibodies: RhoA (1:500 26C4, Santa Cruz), Rac1 (1:1,000 05-389; Upstate Biotechnology, Lake Placid, NY), and Cdc42 (1:500 B-8, Santa Cruz). The level of membrane-bound protein was normalized against the corresponding protein level in whole cell lysates of the respective clones.

Results

Transfections. The breast cancer cell line MDA-MB-468 was stably and transiently transfected with full-length cyclin E COOH-terminally fused to EGFP, or EGFP alone. The generation of stable cyE-overexpressing cells resulted in several clones with various levels of detectable cyE-EGFP fusion protein (Fig. 1*A*). The two clones exhibiting the highest expression, cyE-A10 and cyE-B6, were used together with two control clones (EGFP-B12 and EGFP-G10) in the subsequent experiments.

Flow cytometry. To confirm the established role for cyclin E in cell cycle control, thereby verifying the functionality of the cyclin E construct, flow cytometry was used to assess the cell cycle phase distributions of the transfected populations. The stable clones, cyE-A10 and cyE-B6, and the transiently cyclin E–transfected cells exhibited a significantly increased proportion of cells residing in S phase compared with the control transfectants (Fig. 1*B*). Representative pictures of DNA histograms derived from the stable clones analyzed are shown in Fig. 1*C*.

Oligonucleotide microarray assay. RNA from two cyE-high clones (A10 and B6) and two control clones (B12 and G10)

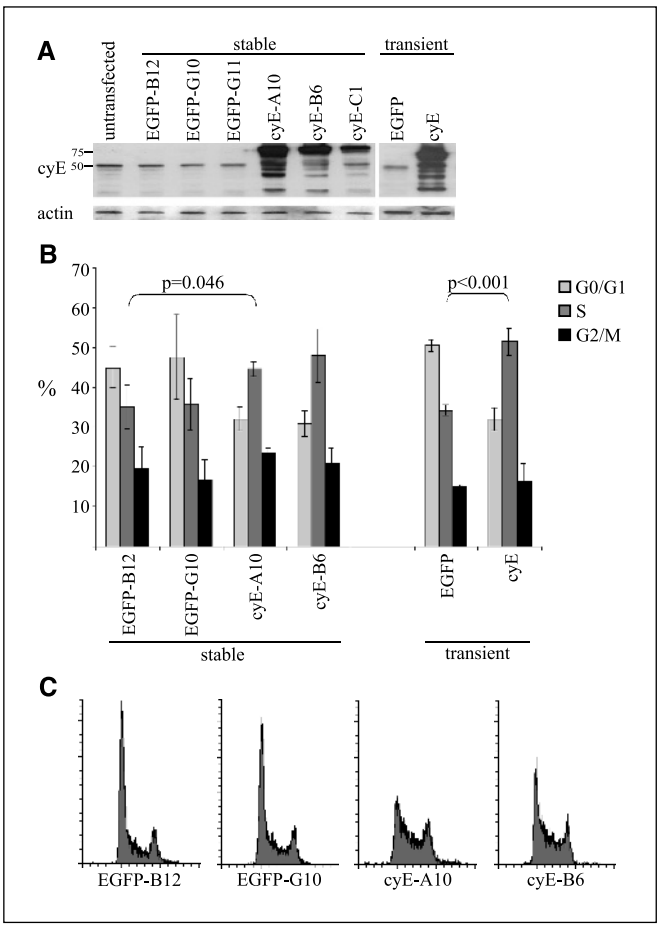

Figure 1. Generation of stable cyclin E–overexpressing clones. *A,* untransfected MDA-MB-468, control-transfected, and cyclin E–transfected cells were harvested and cell lysates were subjected to Western blot analysis with antibodies against cyclin E and actin (loading control). The heavier bands in the cyclin E–transfected clones represent the COOH-terminal fusion protein between cyclin E and EGFP (75 kDa). *B,* ethanol-fixed and propidium iodide–stained cells were analyzed with FACScalibur and Cell Quest software (Becton Dickinson, Franklin Lakes, NJ) for their distribution in different phases of the cell cycle. Average distributions of cells in G_0-G_1-, S-, and G_2-M phases, obtained from at least three independent measurements. SDs are indicated and the P values for the differences in S phase between control clone B12 and cyclin E clone A10 and transient cyclin E– and control-transfected cells were calculated using Students' t test. *C,* representative DNA histograms illustrating the decrease of G_0-G_1 proportion and increase of S-G_2-M-proportion in the cyclin E–overexpressing clones compared with the control clones.

was extracted, reverse-transcribed, and fluorescently labeled. cDNA from the control clones was used as a reference, and was cohybridized to the microarrays together with differentially labeled cDNA from the cyE-high clones. Hybridizations, scanning and data analysis were done as described in Materials and Methods. About 430 genes were found to be transcriptionally affected ≥2-fold by cyclin E overexpression, and 27% of these genes were up-regulated. As expected, cyclin E was one of the genes showing the most pronounced expression difference (~11-fold induction), confirming the reliability of the oligonucleotide microarray. The list of differentially expressed genes was interrogated using the ontologic software GoMiner (11). Classification of the affected genes into biologically coherent categories enabled interpretation of the functional effects of cyclin E overexpression. The GoMiner analysis pointed out several categories containing a significant number of differentially expressed genes (Table 1), including cell proliferation (GO:0008283) and cell adhesion (GO:0007155). A similar ontologic analysis based on microarray experiments using mRNA from transiently transfected MDA-MB-468 cells also indicated cell proliferation (GO:0008283; $P = 0.001$) and cell adhesion molecular activity (GO:0005194; $P = 0.007$) as functional categories being differentially affected in cyclin E– and control–transfected cells. Examples of genes with significantly different expression in the stable cyE-high clones, interesting in the context of the present study are: *THBS1*, ~4.3-fold induction; *PXN*, ~4.5-fold repression; and *MMP7*, ~4.3-fold repression. A clear difference in thrombospondin protein levels between the control clones (B12 and G10) and the cyE-high clones (A10 and B6) was confirmed by immunohistochemical analyses as illustrated in Fig. 3*B*. By manual counting, the fraction of thrombospondin-positive cells was 6% in EGFP-B12 and 27% in cyE-A10. These results were also confirmed by densitometric analysis of the staining intensity (data not shown).

Functional assays. Aiming at defining tumor relevant properties other than proliferation affected by cyclin E deregulation, we investigated whether there were any functional consequences of the differential regulation of genes related to cell adhesion. Adhesive properties of the stable clones were estimated using an MTT-based cell attachment assay. Allowing the cells to adhere for 1 hour, we observed a 30% increase in attachment capability by the cyE-A10 clone compared with the control clones (Fig. 2*A*). Furthermore, we speculated that the cyclin E–mediated change in adhesive properties might manifest itself as an altered ability to migrate and invade. To test this hypothesis, the relative motility of the stable cyE-high clones was determined by conducting a scratch assay. Interestingly, 48 hours after the application of the scratch wound, there was a clear difference in motility between the cyE-high clones and the control clones, indicating an impaired migratory capacity of the cyclin E–overexpressing clones (Fig. 2*B*). We next assessed the effect of cyclin E overexpression on invasive potential by using a Boyden chamber assay. The two cyE-high and control clones, respectively, were pooled in order to simplify the procedure and cells were seeded onto Boyden chambers and allowed to invade. The invasiveness was quantified by manual counting of the invading cells. This experiment showed that the cyclin E–overexpressing cells were significantly less invasive compared with the control cells (Fig. 2*C*). In addition, when analyzing the invasiveness of transiently transfected populations, there was a decreased fraction of invading cells in the cyclin E transfected population compared with the control transfected population (Fig. 2*D*).

Table 1. Genes differentially regulated in cyclin E–transfected clones compared with control clones were classified into biologically coherent categories using the GoMiner software

Gene ontology	Total no. of genes*	No. of differentially expressed genes†	P ‡
Up-regulated genes			
Biological process			
Cell proliferation (8283)	359	16	0.003
Ectoderm development (7398)	29	3	0.021
Molecular function			
Structural molecule activity (5198)	225	11	0.006
Cellular component			
Intermediate filament (5882)	22	4	0.001
Down-regulated genes			
Biological process			
Cell-cell signaling (7267)	131	16	0.004
Cell adhesion (7155)	136	14	0.038
Immune response (6955)	165	16	0.04
Ectoderm development (7398)	29	5	0.025
Molecular function			
Metalloendopeptidase activity (4222)	29	5	0.025
Phosphate metabolism (6796)	226	6	0.028

NOTE: Categories of biological processes, molecular functions, and cellular components including a significant number of genes affected as a result of cyclin E overexpression were annotated according to Gene Ontology terms. The code for each gene ontology term is indicated in parentheses.

*The total number of genes in each category represented on the microarray which passed the filtering criteria.

† The number of differentially expressed genes between cyclin E and control transfected cells.

‡ The Fisher exact test was used in the GoMiner software to calculate the P values for the obtained number of differentially expressed genes in each category.

Cytoskeleton characterization. Several studies have highlighted the importance of the actin cytoskeleton in the formation of active cell-cell adhesions (12), and appropriate cyclic formation-dispersal of cytoskeletal structures is further essential for motility (13). Consequently, we studied the organization of F-actin in the stable clones grown on glass slides, in order to investigate if the decreased mobility of the cyE-high clones was accompanied by, and potentially mediated by, changes in cytoskeletal organization. Using Alexa Fluor 546–conjugated phalloidin staining and immunofluorescence microscopy, we observed that the control clones exhibited a speckled F-actin structure throughout the cell. In contrast, the cyE-high clones exhibited a condensed membrane-associated organization (Fig. 2*E*),

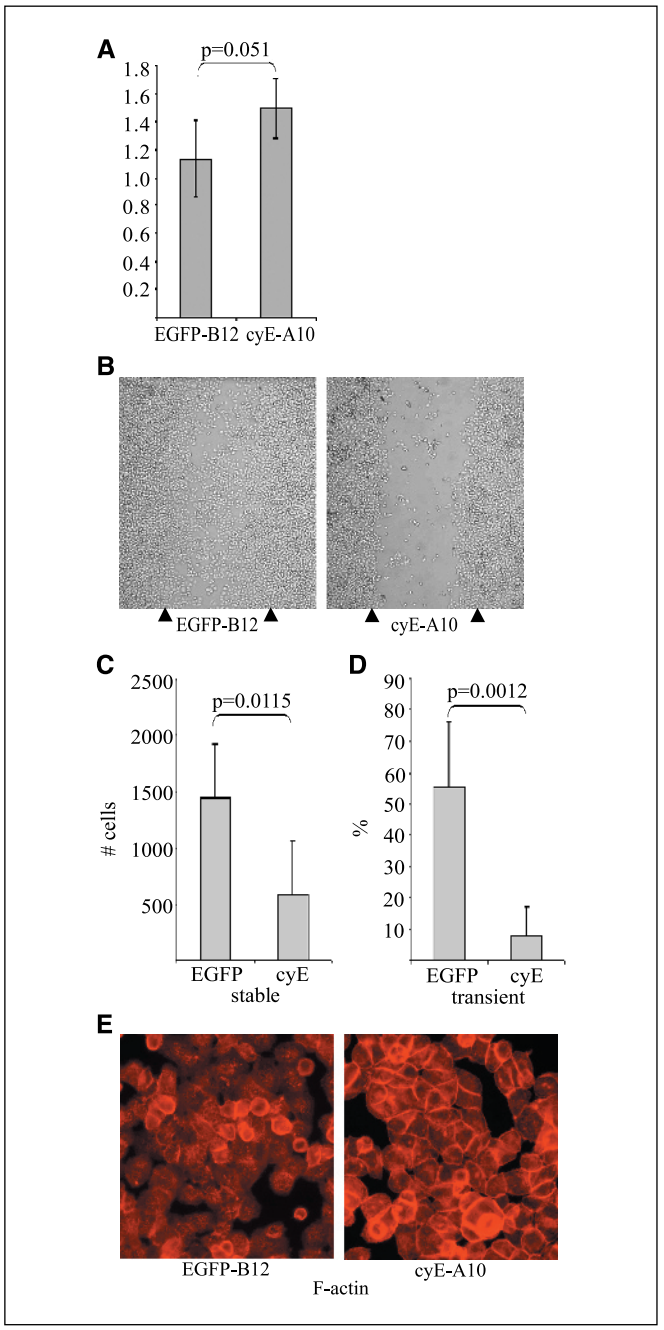

Figure 2. Effects on adhesion-related properties of deregulated cyclin E. *A,* the capacity to adhere was assessed in a cell attachment assay, where the stable clones were allowed to adhere for 1 hour. The amount of attached cells was quantified by absorbance measurements of reduced MTS solution. The adhesion capacity of control clone B12 and cyE-A10, respectively, are shown in relation to control clone G10. *B,* a scratch assay was done to assess the relative mobility of the different clones. Representative photographs are shown for control clone B12 and cyE-A10 48 hours after the application of the scratch; similar results were obtained with clones G10 and B6. *C,* Boyden chamber invasion assay comparing the invasive capacity of control- and cyclin E–transfected clones. The stable control clones and cyclin E clones were pooled, respectively, and plated on top of Matrigel-coated invasion chambers and subsequently allowed to invade towards a serum gradient for 20 hours. The invasive capacity of each pool was measured twice, in triplicate, generating the illustrated average numbers of invading cells and SDs. *D,* the relative invasiveness of the transiently transfected cells was estimated by dividing the proportion of transfected (EGFP-fluorescent) cells among the invading cells with the proportion of transfected cells in a population grown on a control slide. The invasion assay using transiently transfected cells was repeated seven times. Students' *t* test was used to calculate the *P* value. *E,* the actin cytoskeleton organization in cyclin E– and control-transfected clones analyzed by phalloidin staining of F-actin.

indicating a more rigid structure and possibly conferring the less mobile phenotype.

Adhesion/motility-associated proteins. Because it has been shown that E-cadherin/β-catenin complexes mediate the contact between neighboring cells and their actin cytoskeletons (14), we tried to determine whether the change in F-actin cytoskeleton could be due to differences in E-cadherin/β-catenin interactions. We therefore immunoprecipitated E-cadherin and assessed the relative amounts of β-catenin in the corresponding complexes. A comparison of the clones revealed no major differences in the interaction between these two adhesion-related proteins, nor did the total levels of expression differ (Fig. 3*A*). We next focused on p27, a known CDK inhibitor intimately associated with the cyE-CDK2 complex, that has been implemented in regulation of motility by binding to RhoA in the cytoplasm and preventing its activation (15, 16). p27 expression in the control clones (B12 and G10) and the cyE-high clones (A10 and B6) was assessed by immunohistochemistry (Fig. 3*C*), and the fraction of p27-positive cells was 14% and 1.5%, in EGFP-B12 and cyE-A10, respectively (manual counting, validated by densitometric analyses). All p27-positive cells showed a nuclear localization of p27 and cytoplasmic staining could not be observed (Fig. 3*C*). Furthermore, an estimation of the activity of the actin cytoskeleton

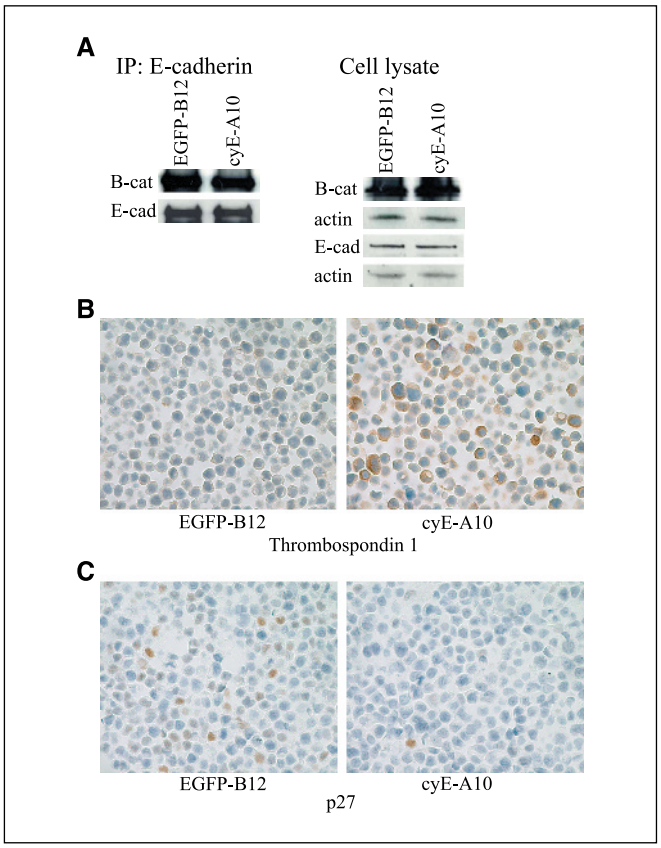

Figure 3. Identification of properties possibly involved in the cyclin E–mediated effect on mobility. *A,* immunoprecipitation of E-cadherin and immunoblotting against E-cadherin and β-catenin (*left*). Total expression of E-cadherin and β-catenin assessed by Western blot using whole cell lysates of the indicated clones. Actin was used as a loading control. *B,* immunohistochemical assessment of *THBS1* using cell pellets of control and cyclin E–transfected clones. An increase in the protein level of *THBS1* was seen in both cyclin E–transfected clones. *C,* cell pellets immunohistochemically stained against p27. Cyclin E–overexpressing clones exhibited an almost negative p27 staining.

regulators RhoA, Rac1, and Cdc42 (17), measured by the relative membrane bound fractions, failed to show any differences between control and cyclin E clones (data not shown). Because there was no obvious change in RhoA activity, it seems unlikely that the phenotypic differences in motility observed between the cyE-high clones and control clones could be explained by altered p27-RhoA interactions.

Analysis of tumor samples. In order to address whether the effect of cyclin E on invasion had any equivalence *in vivo*, we coanalyzed 985 primary breast tumors with regards to cyclin E levels and tumor growth patterns. We hypothesized that if the decreased invasiveness of the cyE-high clones reflected a cyclin E–mediated behavior, then there might be differences in growth patterns between cyE-high and -low tumors. The tumors were arranged in a tissue microarray and cyclin E immunoreactivity was scored as fractions of positive nuclei divided into four groups: 1, 0% to 1%; 2, 2% to 10%; 3, 11% to 50%; and 4, 51% to 100% (Fig. 4*A*). In all of the tumor samples, the cyclin E fractions were distributed as follows: 1, 61%; 2, 20%; 3, 13%; and 4, 6%. In a subset of the entire tumor sample (premenopausal patients, n = 349), cyclin E staining correlated positively with Ki-67 ($P < 0.001$, Spearman's correlation test) and inversely with estrogen receptor and progesterone receptor status (both $P < 0.001$). In addition, there was a significant correlation between cyclin E and *Her2*-amplification ($P < 0.001$), although the correlation to Her2 protein expression (immunohistochemistry) was not as strong ($P = 0.096$). The growth patterns of the tumors were assessed using whole tumor sections and characterized by the mode of infiltration, from a "sieving" and diffuse infiltration to a clearly pushing growth pattern with well-defined margins (Fig. 4*B*). The tumor growth patterns were divided into four groups: 1, infiltrative; 2, infiltrative, pushing features; 3, pushing, infiltrative features; and 4, pushing. In the entire sample, 55 tumors with >50% cyclin E–positive cells were identified, and a majority of these tumors (67%) exhibited a predominantly pushing growth pattern (groups 3 and 4). We randomly selected a similar number of tumors with a lower cyclin E positivity (representing groups 1, 2, and 3, respectively), and their growth patterns were assessed by the same standard. Interestingly, there was a significant difference in the distribution of growth patterns depending on the level of cyclin E expression ($P < 0.001$, calculated using χ^2 test). About 88% of the cyclin E–negative tumors seemed to grow in a clearly infiltrative fashion (Fig. 4*C*). Furthermore, upon examination of the tumors with the most distinct pushing growth pattern (n = 37), 84% had been diagnosed as medullary carcinomas. This tumor type is in part defined by its characteristic solid and delimited growth (18), and among the medullary carcinomas included in the tissue microarrays (n = 40), a majority exhibited high levels of cyclin E (0-1% = 0%, 1-10% = 13%, 10-50% = 30%, and 50-100% = 57%). Considering the high frequency of cyclin E deregulation among medullary tumors, this tumor type clearly differed from the other histologic breast cancer subtypes (Fig. 4*D*).

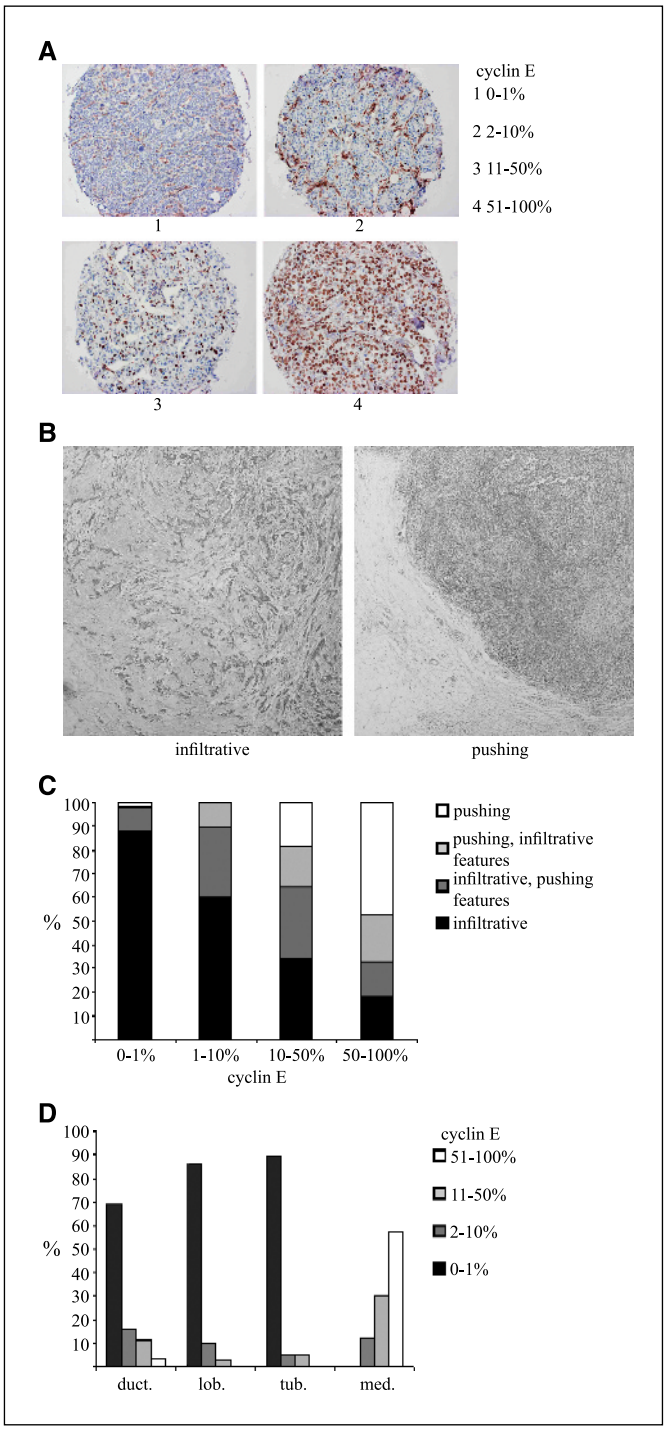

Figure 4. Analysis of breast tumor growth patterns in correlation to cyclin E expression. *A,* immunohistochemically stained tissue microarray sections using an antibody against cyclin E. The cyclin E positivity was assessed based on the fraction of cells with nuclear positivity and represent the four fractions used in the analysis. *B,* tumors growing in an infiltrative (*left*) and pushing manner (*right*). Two intermediate groups with predominantly infiltrative or pushing growth patterns, respectively, were used in addition to the above-exemplified extreme groups. In order to assess growth patterns, whole tissue sections were used. *C,* the distribution of the four growth patterns in tumor groups with increasing levels of cyclin E expression. The total number of tumors in each cyclin E group were: 0% to 1%, 56; 2% to 10%, 57; 11% to 50%, 53; 51% to 100%, 55. The growth pattern distribution in the four cyclin E groups was significantly different ($P < 0.001$, χ^2 test). *D,* cyclin E expression in different histologic breast tumor types; duct., invasive ductal (n = 328); lob., invasive lobular (n = 58); tub., invasive tubular (n = 19); med., medullary (n = 40).

Discussion

Because cyclin E has been implicated in tumorigenic events and is overexpressed in a fraction of breast tumors (19–21), we wanted to obtain a more detailed understanding of the role of cyclin E in breast cancer. The study aimed at exploring functional consequences of cyclin E deregulation other than the well-known

cell cycle regulatory effects. We therefore overexpressed full-length cyclin E in MDA-MB-468 breast cancer cells and analyzed transcriptional changes in order to extract information about affected functions. By using a retinoblastoma-inactivated cell line (22), cyclin E effects unrelated to pRb-phosphorylation could be isolated and investigated. Furthermore, a previous study showed that in MDA-MB-468 cells, cyclin E largely controlled the CDK2 kinase activity, contrasting pRb-normal cell lines where the kinase activity was not as affected by increased levels of cyclin E due to relocalization of the CDK inhibitors p21 and p27 (23). Therefore, by using MDA-MB-468 cells with a nonfunctioning pRb-pathway the cyE-CDK2 activity would be less inhibited, facilitating the detection of cyclin E–dependent downstream effects.

The initial flow cytometry analysis confirmed the ability of the cyE-EGFP fusion protein to influence the cell cycle regulation as expected. It should be noted that in this setting, the effect of cyclin E on triggering G_1-S transition was not dependent on pRb-inactivation and release of E2F. These results stress the importance of the pRb-unrelated functions of cyclin E such as initiation of DNA replication, histone synthesis, and centrosome duplication (24).

The approach of analyzing changes in gene transcription patterns to obtain indications of altered functions (using ontologic mapping) resulted in the hypothesis that cyclin E overexpression might affect adhesion-related properties. In functional assays, we could observe phenotypic changes of the cyE-high clones confirming this hypothesis. Increased attachment capability, decreased motility illustrated in a scratch assay, and furthermore, a lower invasiveness through Matrigel-coated invasion membranes, collectively indicated that overexpression of cyclin E in MDA-MB-468 cells conferred a decreased mobility. The decreased invasiveness of transiently cyclin E–transfected cells strengthened the supposition that the decreased invasive potential of the stable cyE-clones was induced by overexpression of cyclin E and was not a result of clonal variation.

Cytoskeletal structures play a crucial role in cellular activities like cell adhesion and motility (12, 13). Reorganization of the cell architecture is in addition required throughout the cell division cycle, and several reports have indicated a link between the cell cycle machinery and organization of the cytoskeleton (25–27). Stable overexpression of cyclin E in MDA-MB-468 cells did significantly affect the organization of the F-actin cytoskeleton, promoting a membrane-associated condensation that could potentially reflect a more pronounced intercellular adhesion. In an attempt to clarify a mediating link between cyclin E and actin cytoskeletal organization, we analyzed both the E-cadherin/β-catenin complexes and the activity of the actin cytoskeleton regulators RhoA, Rac1, and Cdc42. Surprisingly, no substantial differences in either abundance or activity could be detected.

Other possible contributors to the observed phenotypical changes of the cyE-high clones are likely to be found among the genes differentially expressed in the analyzed clones. Several of the genes included in the functional categories listed in Table 1, might be considered as interesting candidate genes. In the cell adhesion category, we found *THBS1* to be transcriptionally induced ~4-fold (increase of protein level confirmed by immunohistochemistry), a finding which could be of relevance not only regarding adhesion and invasion, but also in vascularization (28–30). In the same category, *PXN*, a gene that has been reported to be a positive regulator of motility (31), was repressed ~4.5-fold. Furthermore, in the category of metalloendopeptidase activity, *MMP7* was shown to be repressed ~4-fold. This latter down-regulation could have implications for the invasive ability of the cyE-high cells (32). Our results indicate that deregulated cyclin E affects several different adhesion- and invasion associated proteins, and it would be of great interest to further investigate underlying molecular mechanisms to the phenotypical alterations. Importantly, the fundamental difference in F-actin organization clearly suggests that the effect of cyclin E on the mobility of MDA-MB-468 cells is mediated through rearrangements of the actin cytoskeleton.

Analyzing the correlation between cyclin E levels and the growth pattern of primary breast tumors corroborated the clinical relevance of the *in vitro* results. Interestingly, we observed a significant association between high levels of cyclin E and a low infiltrative, pushing tumor growth. This association is in agreement with the *in vitro* results showing a decreased invasiveness due to cyclin E overexpression. In the context of tumor biology, it is however, difficult to understand the relation between cyclin E and invasion. CyE-high breast tumors are associated with a poorer prognosis, and, as this study indicates, a large proportion of these tumors grow in a low infiltrative fashion. Because a decreased infiltrative potential would, intuitively, correlate with a better prognosis, our observation implies two seemingly contradictive properties of cyE-high breast tumors. The frequent overexpression of cyclin E in medullary tumors, a tumor type with a relatively good prognosis (18), is an equally puzzling finding. The marked inflammatory response significant for this tumor type could, however, possibly counteract the many aggressive features such as low differentiation grade and high cyclin E levels. The indication that cyclin E affects both tumor-stimulating properties (increased proliferation and chromosome instability) as well as properties presumably delimiting the aggressive nature of tumors (decreased invasive potential), challenges the understanding of the rationale behind the claimed prognostic values of cyclin E. One logical consequence of our results is to introduce a division of the subgroup of cyE-high tumors based on growth pattern. Cyclin E–overexpressing tumors with a pushing growth pattern might have a better prognosis compared with infiltrative cyE-high tumors. If cyclin E is able to affect tumor growth patterns *in vivo*, as our data suggests, then it would be valuable to delineate the different genetic backgrounds allowing cyclin E to exert this influence on a subset of overexpressing tumors.

We have previously observed that infiltrating basal cell carcinomas and colorectal cancer cells display markedly decreased proliferation due to increased p16 expression (33, 34). In the present study, we observed low invasiveness as a consequence of elevated cyclin E levels and an increased fraction of cells in S-G_2-M-phases. These observations support the concept that proliferation and invasion might be two contrasting, and in some instances, incompatible, cellular activities.

Taken together, we report an inverse association between infiltrative growth of primary breast carcinomas and the level of cyclin E expression; an association most clearly reflected in medullary carcinomas. According to our *in vitro* results, this association could be partly due to an obstructed invasive potential induced by overexpression of cyclin E, possibly mediated by an increased cellular adhesion. These results imply a novel, pRb-independent role of cyclin E in modeling adhesive and invasive behavior, in addition to its function in controlling proliferation.

It will be interesting to explore if the intriguing association between cyclin E and infiltrative behavior defined in breast cancer is a general phenomenon which is valid in other malignancies as well.

Acknowledgments

Received 11/8/2004; revised 7/27/2005; accepted 8/18/2005.

Grant support: Swedish Cancer Society, the Gunnar, Arvid, and Elisabeth Nilsson Cancer Foundation, the Royal Physiographical Society of Sweden, Lund University Research Funds, and Malmö University Hospital Research and Cancer Funds. Oligonucleotide microarrays were obtained from the SWEGENE DNA Microarray Resource Center at the Biomedical Center in Lund, supported by the Knut and Alice Wallenberg Foundation through the SWEGENE Consortium. Tissue microarrays were obtained from the National Tissue Array Center in Malmö, supported by the Wallenberg Consortium North through the SWEGENE Consortium. I. Hedenfalk was supported by a postdoctoral fellowship from the Knut and Alice Wallenberg Foundation through the SWEGENE Consortium.

The costs of publication of this article were defrayed in part by the payment of page charges. This article must therefore be hereby marked *advertisement* in accordance with 18 U.S.C. Section 1734 solely to indicate this fact.

We thank Elise Nilsson for excellent technical assistance.

References

1. Putti TC, Abd El-Rehim DM, Rahka EA, et al. Estrogen receptor-negative breast carcinomas: a review of morphology and immunophenotypical analysis. Mod Pathol 2005;18:26–35.
2. WHO. International histological classification of tumours. Histologic types of breast tumours. Geneva: WHO; 1991.
3. Keyomarsi K, Tucker SL, Buchholz TA, et al. Cyclin E and survival in patients with breast cancer. N Engl J Med 2003;348:1566–75.
4. Ohtsubo M, Theodoras AM, Schumacher J, Roberts JM, Pagano M. Human cyclin E, a nuclear protein essential for the G1-to-S phase transition. Mol Cell Biol 1995;15: 2612–24.
5. Resnitzky D, Gossen M, Bujard H, Reed SI. Acceleration of the G1/S phase transition by expression of cyclins D1 and E with an inducible system. Mol Cell Biol 1994;14:1669–79.
6. Ekholm-Reed S, Mendez J, Tedesco T, Zetterberg A, Stillman B, Reed SI. Deregulation of cyclin E in human cells interferes with prereplication complex assembly. J Cell Biol 2004;165:789–800.
7. Kawamura K, Izumi H, Ma Z, et al. Induction of centrosome amplification and chromosome instability in human bladder cancer cells by p53 mutation and cyclin E overexpression. Cancer Res 2004;64:4800–9.
8. Bortner DM, Rosenberg MP. Induction of mammary gland hyperplasia and carcinomas in transgenic mice expressing human cyclin E. Mol Cell Biol 1997;17:453–9.
9. Sutherland RL, Musgrove EA. Cyclins and breast cancer. J Mammary Gland Biol Neoplasia 2004;9:95–104.
10. Saal LH, Troein C, Vallon-Christersson J, Gruvberger S, Borg A, Peterson C. BioArray Software Environment (BASE): a platform for comprehensive management and analysis microarray data. Genome Biol 2002;15: Software 0003.
11. Zeeberg BR, Feng W, Wang G, et al. GoMiner: a resource for biological interpretation of genomic and proteomic data. Genome Biol 2003;4:R28.
12. Vasioukhin V, Fuchs E. Actin dynamics and cell-cell adhesion in epithelia. Curr Opin Cell Biol 2001;13: 76–84.
13. Kodama A, Lechler T, Fuchs E. Coordinating cytoskeletal tracks to polarize cellular movements. J Cell Biol 2004;167:203–7.
14. Perez-Moreno M, Jamora C, Fuchs E. Sticky business: orchestrating cellular signals at adherens junctions. Cell 2003;21:535–48.
15. Besson A, Gurian-West M, Schmidt A, Hall A, Roberts RM. p27Kip1 modulates cell migration through the regulation of RhoA activation. Genes Dev 2004;18: 862–76.
16. Vlach J, Hennecke S, Amati B. Phosphorylation-dependent degradation of the cyclin-dependent kinase inhibitor p27. EMBO J 1997;16:5334–44.
17. Nobes CD, Hall A. Rho GTPases control polarity, protrusion, and adhesion during cell movement. J Cell Biol 1999;144:1235–44.
18. Pedersen L. Medullary carcinoma of the breast. APMIS Suppl 1997;75:1–31.
19. Spruck CH, Won KA, Reed SI. Deregulated cyclin E induces chromosome instability. Nature 1999;401: 297–300.
20. Nielsen NH, Arnerlov C, Emdin SO, Landberg G. Cyclin E overexpression, a negative prognostic factor in breast cancer with strong correlation to oestrogen receptor status. Br J Cancer 1996;74:874–80.
21. Kuhling H, Alm P, Olsson H, et al. Expression of cyclin E, A and B, and prognosis in lymph node-negative breast cancer. J Pathol 2003;199:424–31.
22. Lee EY, To H, Shew JY, Bookstein R, Scully P, Lee WH. Inactivation of the retinoblastoma susceptibility gene in human breast cancers. Science 1988;8:218–21.
23. Lodén M, Stighall M, Nielsen NH, et al. The cyclin D1 high and cyclin E high subgroups of breast cancer: separate pathways in tumorigenesis based on pattern of genetic aberrations and inactivation of the pRb node. Oncogene 2002;21:4680–90.
24. Ewen ME. Where the cell cycle and histones meet. Genes Dev 2000;15:2265–70.
25. Besson A, Assoian RK, Roberts JM. Regulation of the cytoskeleton: an oncogenic function for CDK inhibitors? Nat Rev Cancer 2004;4:948–55.
26. Manes T, Zheng DQ, Tognin S, Woodard AS, Marchisio PC, Languino LR. α(v)β3 integrin expression up-regulates cdc2, which modulates cell migration. J Cell Biol 2003;161:817–26.
27. Neumeister P, Pixley FJ, Xiong Y, et al. Cyclin D1 governs adhesion and motility of macrophages. Mol Biol Cell 2003;14:2005–15.
28. Adams JC. Thrombospondins: multifunctional regulators of cell interactions. Annu Rev Cell Dev Biol 2001; 17:25–51.
29. Weinstat-Saslow DL, Zabrenetzky VS, VanHoutte K, Frazier WA, Roberts DD, Steeg PS. Transfection of thrombospondin 1 complementary DNA into a human breast carcinoma cell line reduces primary tumor growth, metastatic potential, and angiogenesis. Cancer Res 1994;54:6504–11.
30. Manni A, Washington S, Mauger D, Hackett DA, Verderame MF. Cellular mechanisms mediating the anti-invasive properties of ornithine decarboxylase inhibitor α-difluoromethylornithine (DFMO) in human breast cancer cells. Clin Exp Metastasis 2004;21:461–7.
31. Hagel M, George EL, Kim A, et al. The adaptor protein paxillin is essential for normal development in the mouse and is a critical transducer of fibronectin signaling. Mol Cell Biol 2002;22:901–15.
32. Shiomi T, Okada Y. MT1-MMP and MMP-7 in invasion and metastasis in human cancers. Cancer Metastasis Rev 2003;22:145–52.
33. Svensson S, Nilsson K, Ringberg A, Landberg G. Invade or proliferate? Two contrasting events in malignant behavior governed by p16 (INK4a) and an intact Rb pathway illustrated by a model system of basal cell carcinoma. Cancer Res 2003;15:1737–42.
34. Palmquist R, Rutegard JN, Bozoky B, Landberg G, Stenling R. Human colorectal cancers with an intact p16/cyclin D1/ pRb pathway have up-regulated p16 expression and decreased proliferation in small invasive tumor clusters. Am J Pathol 2000;157:1947–53.

Cyclin E Overexpression Obstructs Infiltrative Behavior in Breast Cancer: A Novel Role Reflected in the Growth Pattern of Medullary Breast Cancers

Pontus Berglund, Maria Stighall, Karin Jirström, et al.

Cancer Res 2005;65:9727-9734.